Ab Initio Studies of the Contrasting Butadiene Cheletropic and Diels−Alder Cycloaddition Reactivities Observed for "Carbenic" Phosphorus (Phosphenium) and Arsenic (Arsenium) Cations†

Russell J. Boyd, Neil Burford,* and Charles L. B. Macdonald

Department of Chemistry, Dalhousie University, Halifax, Nova Scotia, Canada B3H 4J3

Received February 23, 1998

Quantum-chemical studies (UMP2/6-311G*//UHF/6-311G*) on a series of phosphenium and arsenium derivatives confirm singlet ground states and reveal an unexpected model for the bonding in their lowest triplet state. Models of the novel solid-state dimer structures that are experimentally observed for some arsolanium cations reveal large positive dimerization energies (P, **3**, 277 kJ/mol; As, **7**, 207 kJ/mol), implying that the observed dimers are imposed by crystal-packing phenomena. The surprising contrast observed in the butadiene cycloaddition reactivities for phosphenium and arsenium cations are understood in terms of the calculated absolute energies of the observed structural arrangements for the cycloadducts in each case; the cheletropic adduct **4** is 52 kJ/mol more stable than the Diels−Alder adduct for the phospholanium cation, while in the case of the arsolanium cation the Diels−Alder adduct **9** is favored by 59 kJ/mol.

Introduction

Interest in carbenes **1a** and the analogous systems **1** and **2** stems from their intriguing electronic structure, fascinating reactivity (e.g. electrophilic and nucleophilic behavior and as ligands in homogeneous catalysts (achiral and chiral[1)2]), and corresponding synthetic utility.[3−6] Isolable examples are known for carbenes

1 **a:** E = C **b:** E = Si **c:** E = Ge **d:** E = Sn **e:** E = Pb

2 **a:** Pn = N **b:** Pn = P **c:** Pn = As **d:** Pn = Sb **e:** Pn = Bi

(**1a**),[4,7−10] silylenes (**1b**),[11] germylenes (**1c**),[11,12] stannylenes (**1d**),[11,12] and plumbylenes (**1e**)[13] as well as for

* To whom correspondence should be addressed. E-mail: burford@is.dal.ca.

† This article is dedicated to Prof. Dr. Peter Jutzi on the occasion of his 60th birthday.

(1) See for example: (a) Herrmann, W. A.; Goossen, L. J.; Artus, G. R. J.; Köcher, C. *Organometallics* **1997**, *16*, 2472−2477. (b) Hermann, W. A.; Goossen, L. J.; Spiegler, M. *J. Organomet. Chem.* **1997**, *547*, 357−366.

(2) (a) Herrmann, W. A.; Elison, M.; Fischer, J.; Köcher, C.; Artus, G. R. J. *Angew. Chem., Int. Ed. Engl.* **1995**, *34*, 2371−2374. (b) Herrmann, W. A.; Köcher, C. *Angew. Chem., Int. Ed. Engl.* **1997**, *36*, 2162−2187.

(3) For a compendium of transient carbenoids see: Nefedov, O. M.; Egorov, M. P.; Ioffe, A. I.; Menchikov, L. G.; Zuev, P. S.; Minikin, V. I.; Simkin, B. Y.; Glukhovtsev, M. N. *Pure Appl. Chem.* **1992**, *64*, 265−314.

(4) Regitz, M. *Angew. Chem., Int. Ed. Engl.* **1996**, *35*, 725−728 and references therein.

(5) *Houben-Weyl, Methoden der Organischen Chemie*; Regitz, M., Ed.; Thieme: Stuttgart, Germany, 1989; Part 2, Vol. E19b.

(6) Driess, M.; Grützmacher, H. *Angew. Chem., Int. Ed. Engl.* **1996**, *35*, 828−856.

(7) Arduengo, A. J., III.; Harlow, R. L.; Kline, M. *J. Am. Chem. Soc.* **1991**, *113*, 361−363.

(8) For example: (a) Dixon, D. A.; Arduengo, A. J., III. *J. Phys. Chem.* **1991**, *95*, 4180−4182. (b) Arduengo, A. J., III.; Dias, H. V. R.; Harlow, R. L.; Kline, M. *J. Am. Chem. Soc.* **1992**, *114*, 5530−5534. (c) Arduengo, A. J., III; Dixon, D. A.; Kumashiro, K. K.; Lee, C.; Power, W. P.; Zilm, K. W. *J. Am. Chem. Soc.* **1994**, *116*, 6361−6367. (d) Arduengo, A. J., III; Bock, H.; Chen, H.; Denk, M.; Dixon, D. A.; Green, J. C.; Herrmann, W. A.; Jones, N. L.; Wagner, M.; West, R. *J. Am. Chem. Soc.* **1994**, *116*, 6641−6649. (e) Arduengo, A. J., III; Dias, H. V. R.; Dixon, D. A.; Harlow, R. L.; Klooster, W. T.; Koetzle, T. F. *J. Am. Chem. Soc.* **1994**, *116*, 6812−6822. (f) Arduengo, A. J., III; Goerlich, J. R.; Marshall, W. J. *J. Am. Chem. Soc.* **1995**, *117*, 11027−11028. (g) Arduengo, A. J., III; Calabrese, J. C.; Cowley, A. H.; Dias, H. V. R.; Goerlich, J. R.; Marshall, W. J.; Riegel, B. *Inorg. Chem.* **1997**, *36*, 2151−2158. (h) Arduengo, A. J., III; Davidson, F.; Dias, H. V. R.; Goerlich, J. R.; Khasnis, D.; Marshall, W. J.; Prakasha, T. K. *J. Am. Chem. Soc.* **1997**, *119*, 12742−12749. (i) Arduengo, A. J., III; Goerlich, J. R.; Marshall, W. J. *Liebigs Ann./Recl.* **1997**, 365−374.

(9) Alder, R. A.; Allen, P. R.; Murray, M.; Orpen, A. G. *Angew. Chem., Int. Ed. Engl.* **1996**, *35*, 1121−1123.

(10) Denk, M. K.; Thadani, A.; Hatano, K.; Lough, A. J. *Angew. Chem., Int. Ed. Engl.* **1997**, *36*, 2607−2609.

(11) Tsumuraya, T.; Batcheller, S. A.; Masamune, S. *Angew. Chem., Int. Ed. Engl.* **1991**, *30*, 902−930.

(12) Neumann, W. P. *Chem. Rev.* **1991**, *91*, 311−334.

(13) See, for example: (a) Brooker, S.; Buijink, J.-K.; Edelmann, F. T. *Organometallics* **1991**, *10*, 25−26. (b) Gehrhus, B.; Hitchcock, P. B.; Lappert, M. F. *Angew. Chem., Int. Ed. Engl.* **1997**, *36*, 2514−2516.

(14) Sanchez, M.; Mazières, M.-R.; Lamandé, L.; Wolf, R. *Multiple Bonds and Low Coordination in Phosphorus Chemistry*; Regitz, M., Sherer, O. J., Eds.; Thieme: New York, 1990; pp 129−148.

(15) (a) Flemming, S.; Lupton, M. K.; Jekot, K. *Inorg. Chem.* **1972**, *11*, 2534−2540. (b) Maryanoff, B. E.; Hutchins, R. O. *J. Org. Chem.* **1972**, *37*, 3475−3480.

(16) Burford, N.; Losier, P.; Macdonald, C.; Kyrimis, V.; Bakshi, P. K.; Cameron, T. S. *Inorg. Chem.* **1994**, *33*, 1434−1439.

(17) For example: (a) Burford, N.; Royan, B. W.; White, P. S. *J. Am. Chem. Soc.* **1989**, *111*, 3746−3747. (b) Burford, N.; Parks, T. M.; Royan, B. W.; Richardson, J. F.; White, P. S. *Can. J. Chem.* **1992**, *70*, 703−709. (c) Veith, M.; Bertsch, B.; Huch, V. *Z. Anorg. Allg. Chem.* **1988**, *559*, 73−88. (d) Payrastre, C.; Madaule, Y.; Wolf, J.-G. *Tetrahedron Lett.* **1992**, *33*, 1273−1276. (e) Payrastre, C.; Madaule, Y.; Wolf, J.-G.; Kim, T. C.; Mazières, M.-R.; Wolf, R.; Sanchez, M. *Heteroat. Chem.* **1992**, *3*, 157−162. (f) Burford, N.; Royan, B. W. *J. Chem. Soc., Chem. Commun.* **1989**, 19−21.

S0276-7333(98)00126-5 CCC: $15.00
Publication on Web 08/12/1998

the cationic group 15 analogues phosphenium (**2b**),[14−16] arsenium (**2c**),[17−20] stibenium (**2d**),[21] and bismuthenium (**2e**).[22] All structural studies of pnictogenium cations reveal monomeric units in the solid state except in the case of arsolidinium salts **7′** (and the dithia derivatives) which adopt dimeric solid-state structures **10′**.[19] The observation of a monomeric structure for the arsenanium salt **11′**[$GaCl_4$] implies a small (if any) dimerization energy for **7′**.[18] A more dramatic contrast is apparent between phosphorus and arsenic analogues in the rapid, regiospecific, and quantitative cycloaddition reactions of salts **3′**[$GaCl_4$] and **7′**[$GaCl_4$] with 2,3-dimethylbutadiene, which give the spirocyclic cation salts **4′**[$GaCl_4$][23] and the Diels−Alder type product **9′**-[$GaCl_4$],[20] respectively (**11′**[$GaCl_4$] reacts analogously).[18]

A rationale for the solid-state structural differences of group 14 and 15 carbene analogues has recently been described in the context of the Carter-Goddard-Malrieu-Trinquier model (CGMT);[6] however, reactivity differences have not been addressed. In an attempt to understand the factors governing the structure and the cycloaddition behavior of cations **3′** and **7′**, we have performed quantum-chemical investigations of model cations **3** and **7**, confirmed the singlet ground state multiplicity, and determined the thermodynamically preferred products for cycloaddition reactions with butadiene through the examination of potential cycloadducts.[16,19,23]

Theoretical Methods and Results

All calculations were performed on an IBM RS6000/580 workstation using the Gaussian94 set of programs.[24] The geometry of each species was optimized by the Hartree−Fock method using the 6-311G* basis set, and all energies were calculated using full second-order Møller−Plesset perturbation theory with the 6-311G* basis set. Model compounds were restricted to the highest appropriate symmetry; optimized structures are displayed in Figures 1 and 2, and structural parameters are listed in Tables 2 and 3[66] (see also Chart 1). All energy minima were confirmed by $3N - 6$ positive eigenvalues of the Hessian matrixes, and the total energies include the HF/6-311G* zero-point vibrational energies (MP2/6-311G*//HF/6-311G* + 0.9 ZPVE (HF)) which are listed in Table 1.[66] Molecular orbital (MO) analyses, spin densities, and charge distributions were determined through the use of Mulliken population analysis and natural bond orbital analysis[25] (NBO), the results of which are listed in Tables 4 and 5.[66]

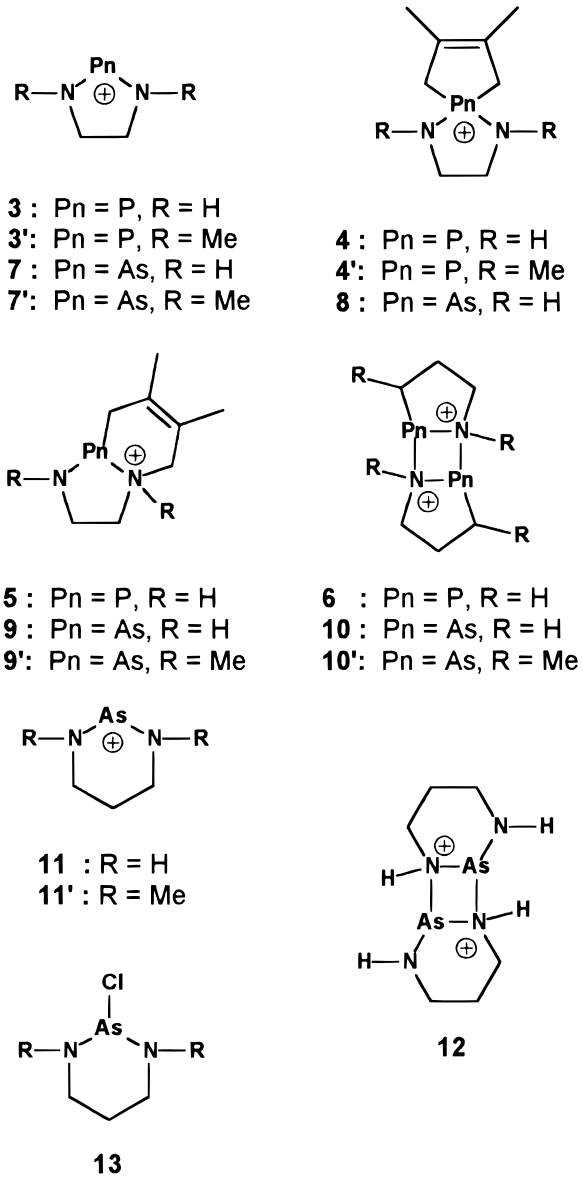

Discussion

Multiplicity of the Ground State for Diazaphosphenium and Diazaarsenium Cations. Various

(18) Burford, N.; Macdonald, C. L. B.; Parks, T. M.; Wu, G.; Borecka, B.; Kwiatkowski, W.; Cameron, T. S. *Can. J. Chem.* **1996**, *74*, 2209−2216.

(19) Burford, N.; Parks, T. M.; Royan, B. W.; Borecka, B.; Cameron, T. S.; Richardson, J. F.; Gabe, E. J.; Hynes, R. *J. Am. Chem. Soc.* **1992**, *114*, 8147−8153.

(20) Burford, N.; Parks, T. M.; Bakshi, P. K.; Cameron, T. S. *Angew. Chem., Int. Ed. Engl.* **1994**, *33*, 1267−1268.

(21) (a) Coleman, A. P.; Nieuwenhuyzen, M.; Rutt, H. N.; Seddon, K. R. *J. Chem. Soc., Chem. Commun.* **1995**, 2369−2370. (b) Neuhaus, A.; Frenzen, G.; Pebler, J.; Dehnicke, K. *Z. Anorg. Allg. Chem.* **1992**, *618*, 93−97.

(22) See for example: (a) Frank, W.; Weber, J.; Fuchs, E. *Angew. Chem., Int. Ed. Engl.* **1987**, *26*, 74−75. (b) Alcock, N. W.; Ravindran, M.; Willey, G. R. *J. Chem. Soc., Chem. Commun.* **1989**, 1063−1065. (c) Rogers, R. D.; Bond, A. H.; Aguinaga, S.; Reyes, A. *J. Am. Chem. Soc.* **1992**, *114*, 2967−2977. (d) Clegg, W.; Farrugia, L. J.; McCamley, A.; Norman, N. C.; Orpen, A. G.; Pickett, N. L.; Stratford, S. E. *J. Chem. Soc., Dalton Trans.* **1993**, 2579−2587. (e) Allman, T.; Goel, R. G.; Prasad, H. S. *J. Organomet. Chem.* **1979**, *166*, 365−371. (f) Carmalt, C. J.; Norman, N. C.; Orpen, A. G.; Stratford, S. E. *J. Organomet. Chem.* **1993**, *460*, C22−C24. (g) Agocs, L.; Burford, N.; Cameron, T. S.; Curtis, J. M.; Richardson, J. F.; Robertson, K. N.; Yhard, G. B. *J. Am. Chem. Soc.* **1996**, *118*, 3225−3232. (h) Agocs, L.; Briand, G. G.; Burford, N.; Cameron, T. S.; Kwiatkowski, W.; Robertson, K. N. *Inorg. Chem.* **1997**, *36*, 2855−2860.

(23) See for example: (a) SooHoo, C. K.; Baxter, S. G. *J. Am. Chem. Soc.* **1983**, *105*, 7443−7444. (b) Cowley, A. H.; Kemp, R. A.; Lasch, J. G.; Norman, N. C.; Stewart, C. A. *J. Am. Chem. Soc.* **1983**, *105*, 7444−7445. (c) Cowley, A. H.; Kemp, R. A.; Lasch, J. G.; Norman, N. C.; Stewart, C. A.; Whittlesey, B. R.; Wright, T. C. *Inorg. Chem.* **1986**, *25*, 740−749.

(24) Frisch, M. J.; Trucks, G. W.; Schlegel, H. B.; Gill, P. M. W.; Johnson, B. G.; Robb, M. A.; Cheeseman, J. R.; Keith, T. A.; Petersson, G. A.; Montgomery, J. A.; Raghavachari, K.; Al-Laham, M. A.; Zakrewski, V. G.; Ortiz, J. V.; Foresman, J. B.; Cioslowski, J.; Stefanow, B. B.; Nanayakkara, A.; Challacombe, M.; Peng, C. Y.; Ayala, P. Y.; Chen, W.; Wong, M. W.; Andres, J. L.; Replogle, E. S.; Gomperts, R.; Martin, R. L.; Fox, D. J.; Binkley, J. S.; DeFrees, D. J.; Baker, J.; Stewart, J. P.; Head-Gordon, M.; Gonzalez, C.; Pople, J. A. GAUSSIAN 94 (Revision B.2); Gaussian, Inc., Pittsburgh, PA, 1995.

(25) Reed, A. E.; Curtis, L. A.; Weinhold, F. *Chem. Rev.* **1988**, *88*, 899−926.

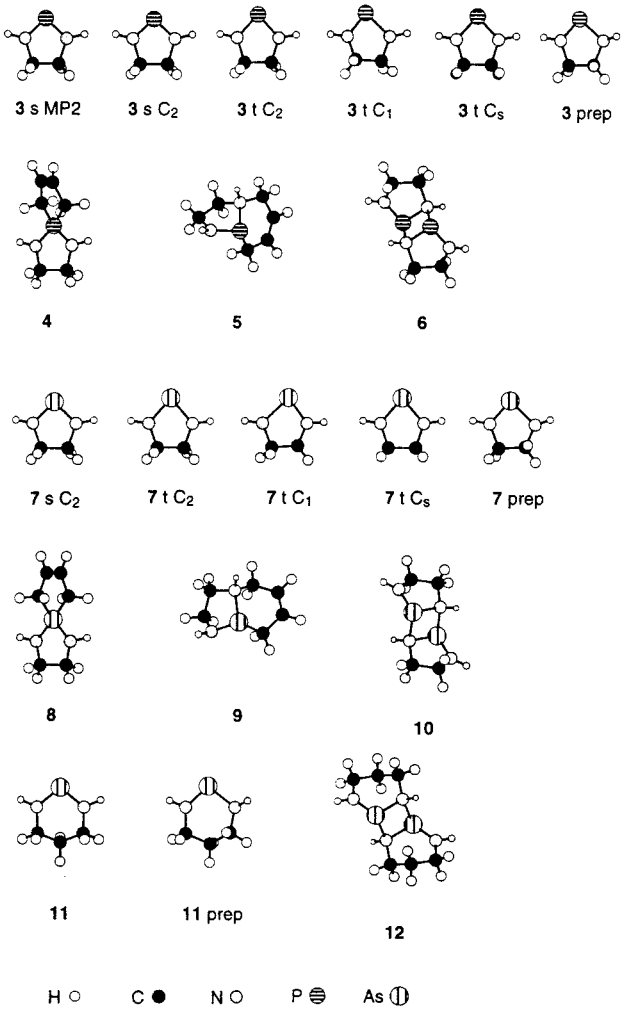

Figure 1. Schematic representations of the HF/6-311G* optimized structures of the cyclic phosphorus and arsenic cations.

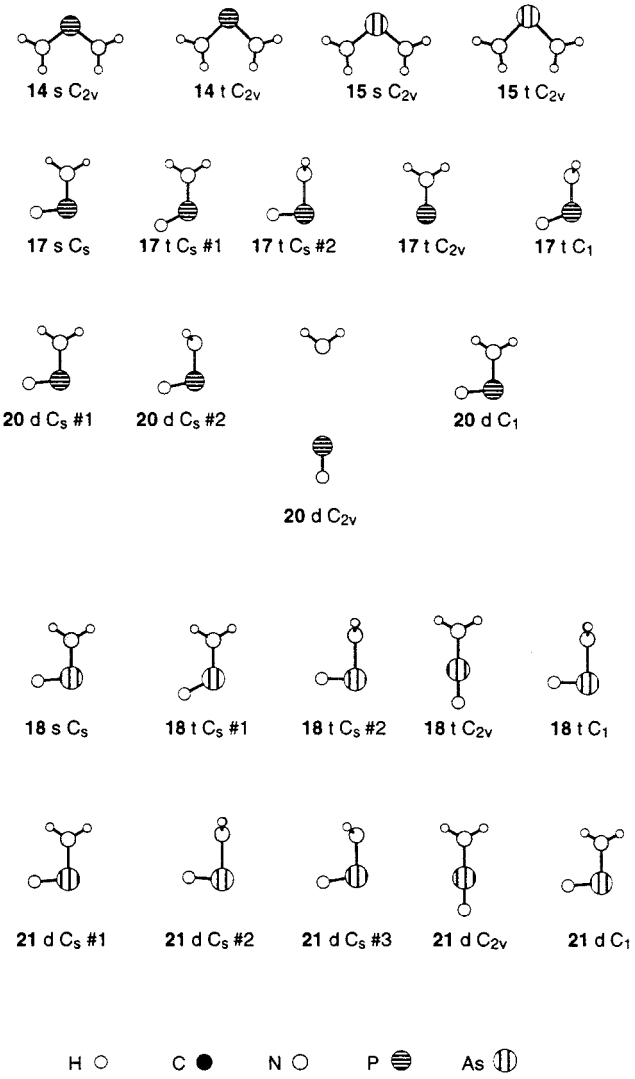

Figure 2. Schematic representations of the HF/6-311G* optimized structures of the acyclic phosphorus and arsenic cations and radicals (H(3) atom not shown in **17** t C_{2v}).

factors govern the stability of pnictogen salts, including the solvent, the presence of base stabilization (inter- or intramolecular), the nature of the counteranion, and the steric and electronic influence of the substituents adjacent to the dicoordinate site. The relative stabilities of such compounds may be assessed by the measurement of the lifetimes of species and their resistance to rearrangement or addition reactions. The isolation of $[GaCl_4]$ or $[AlCl_4]$ salts of pnictogenium cations **2** is perhaps surprising in view of typical Lewis adduct chemistry ($R_2ClPn \rightarrow ECl_3$) of phosphines and arsines but is indicative of the significance of the crystal lattice energy term in defining their stability.[16] Studies using conventional *ab initio* methods typically ignore these external factors; however, such studies do yield insight regarding the inherent stability of such species and thus may be extremely valuable in the understanding of results observed experimentally.

Several topical quantum-chemical studies of ylidenes **1** have provided substantial insight into their structure and bonding.[26−28] Electronic structure models have also been established for the group 15 carbene analogues **2**,[29−37] which indicate that most, including those possessing adjacent π-electron-donor substituents, have a singlet ground state ($[NH_2]^+$ is an exception).[38] In this context, we have performed full geometry optimizations and frequency calculations at the HF/6-311G* level of theory for model cations **3** and **7** with singlet (C_2 symmetry) and triplet ground states (C_1, C_2, C_s, and C_{2v}

(26) Heinemann, C.; Müller, T.; Apeloig, Y.; Schwarz, H. *J. Am. Chem. Soc.* **1996**, *118*, 2023−2038.
(27) Boehme, C.; Frenking, G. *J. Am. Chem. Soc.* **1996**, *118*, 2039−2046.
(28) Sauers, R. R. *Tetrahedron Lett.* **1996**, *37*, 149−152.
(29) Cowley, A. H.; Cushner, M. C.; Lattman, M.; McKee, M. L.; Szobota, J. S.; Wilburn, J. C. *Pure Appl. Chem.* **1980**, *52*, 789−797.
(30) Harrison, J. F. *J. Am. Chem. Soc.* **1981**, *103*, 7406−7413.
(31) Trinquier, G.; Marre, M.-R. *J. Phys. Chem.* **1983**, *87*, 1903−1905.
(32) Cramer, C. J.; Dulles, F. J.; Storer, J. W.; Worthington, S. E. *Chem. Phys. Lett.* **1994**, *218*, 387−394.
(33) MacLennan, M. T.; Darvesh, K. V. *Can. J. Chem.* **1995**, *73*, 544−549.
(34) Sauers, R. R. *Tetrahedron* **1997**, *53*, 2357−2364.
(35) Latifzadeh-Masoudipour, L.; Balasubramanian, K. *J. Chem. Phys.* **1997**, *106*, 2695−2701.
(36) Latifzadeh, L.; Balasubramanian, K. *Chem. Phys. Lett.* **1996**, *258*, 393−399.
(37) Schoeller, W. W.; Tubbesing, U. *J. Mol. Struct.* **1995**, *343*, 49−55.
(38) See for example: (a) Ford, G. P.; Scribner, J. D. *J. Am. Chem. Soc.* **1981**, *103*, 4281−4291. (b) Falvey, D. E.; Cramer, C. J. *Tetrahedron Lett.* **1992**, *33*, 1705−1708. (c) Su, K.; Hu, X.; Li, X.; Wang, Y.; Wen, Z. *Chem. Phys. Lett.* **1996**, *258*, 431−435. (d) Cramer, C. J.; Falvey, D. E. *Tetrahedron Lett.* **1997**, *38*, 1515−1518.

Table 1. Computed Energies (HF/6-311G* and MP2/6-311G*//HF/6-311G*) and Zero Point Vibrational Energies for all Calculations[a]

cyclic P cation	sym	*N*(imag)	HF	MP2	ZPVE	rel energy
3	C_2	0	−528.695 28	−529.405 88	0.099 15	0.00
3 MP2 optimization	C_2	n/a	n/a	−529.408 49	n/a	
3 t	C_2	1	−528.610 35	−529.291 22	0.093 64	288.02
3 t	C_1	0	−528.617 21	−529.285 10	0.095 13	307.60
3 t	$C_s \rightarrow C_{2v}$*	2	−528.609 95	−529.290 06	0.093 27	290.20
3 prep	C_1	0	−528.658 20	−529.379 05	0.097 58	66.76
4	C_1	0	−683.701 30	−684.948 74	0.194 50	0.00
5	C_1	0	−683.676 14	−684.933 09	0.198 93	51.54
6	C_i	0	−1057.2 6550	−1058.7 0949	0.202 07	
cyclic As cation	sym	*N*(imag)	HF	MP2	ZPVE	rel energy
7	C_2	0	−2422.0 8739	−2422.8 0044	0.097 42	0.00
7 t	C_2	1	−2422.0 2870	−2422.7 0568	0.092 73	237.71
7 t	C_1	0	−2422.0 3716	−2422.7 0234	0.093 85	249.14
7 t	$C_s \rightarrow C_{2v}$*	2	−2422.0 2819	−2422.7 0450	0.092 44	240.14
7 prep	C_1	0	−2422.0 6038	−2422.7 8217	0.096 29	45.28
8	C_1	0	−2577.0 6294	−2578.3 1324	0.192 31	58.53
9	C_1	0	−2577.0 8024	−2578.3 3994	0.197 21	0.00
10	C_i	0	−4844.0 7839	−4845.5 2502	0.198 04	
11	C_s	0	−2461.1 3855	−2461.9 9164	0.128 73	0.00
11 prep	C_1	0	−2461.1 0696	−2461.9 6700	0.127 26	61.22
12	C_i	0	−4922.1 6511	−4923.8 9126	0.260 13	
butadiene	sym	*N*(imag)	HF	MP2	ZPVE	rel energy
cis	C_{2v}	1	−154.942 71	−155.470 37	0.090 46	15.02
trans	C_{2h}	0	−154.949 27	−155.476 36	0.090 76	0.00
ammonia	sym	*N*(imag)	HF	MP2	ZPVE	rel energy
16 s	C_{3v}	0	−56.200 97	−56.380 03	0.037 22	0.00
16 s	D_{3h}	1	−56.190 88	−56.370 79	0.035 14	19.32
16 t	D_{3h}	0	−56.014 11	−56.171 62	0.022 05	511.34
ammonium radical cation	sym	*N*(imag)	HF	MP2	ZPVE	rel energy
19 d	$C_{3v} \rightarrow D_{3h}$[b]	0	−55.888 74	−56.027 26	0.035 15	0.05
19 d	D_{3h}	0	−55.888 74	−56.027 27	0.035 14	0.00
acyclic P cation	sym	*N*(imag)	HF	MP2	ZPVE	rel energy
17 s	C_s	0	−396.669 06	−396.939 72	0.039 08	0.00
17 t	C_s #1	1	−396.593 85	−396.836 97	0.034 44	258.79
17 t	C_s #2	0	−396.619 87	−396.845 50	0.034 81	237.26
17 t	C_{2v}	1	−396.575 80	−396.827 33	0.028 03	268.96
17 t	C_1	0	−396.614 08	−396.861 93	0.034 73	193.94
acyclic P radical	sym	*N*(imag)	HF	MP2	ZPVE	rel energy
20 d	C_s #1	1	−396.922 42	−397.189 02	0.035 22	0.00
20 d	C_s #2	1	−396.913 02	−397.174 84	0.035 06	36.84
20 d	C_{2v}	2	−396.854 40	−397.067 81	0.026 53	297.72
20 d	C_1	0	−396.922 70	−397.189 05	0.036 07	1.92
acyclic As cation	sym	*N*(imag)	HF	MP2	ZPVE	rel energy
18 s	C_s	0	−2290.0 8183	−2290.3 5103	0.037 11	0.00
18 t	C_s #1	2	−2290.0 0474	−2290.2 4755	0.032 42	260.60
18 t	C_s #2	0	−2290.0 5075	−2290.2 6943	0.033 18	204.95
18 t	C_{2v}	3	−2289.9 4675	−2290.1 9220	0.030 58	401.58
18 t	C_1	0	−2290.0 5075	−2290.2 6944	0.033 18	204.94
acyclic As radical	sym	*N*(imag)	HF	MP2	ZPVE	rel energy
21 d	C_s #1	1	−2290.3 3776	−2290.6 0318	0.033 65	0.20
21 d	C_s #2	1	−2290.2 6276	−2290.5 0515	0.031 69	252.94
21 d	C_s #3	1	−2290.3 3260	−2290.5 9418	0.033 86	24.33
21 d	C_{2v}	2	−2290.1 6059	−2290.4 4008	0.041 94	448.03
21 d	C_1	0	−2290.3 3903	−2290.6 0427	0.034 78	0.00

[a] Absolute energies are in hartrees. *N*(imag) indicates the number of imaginary vibrational frequencies. Relative energies (MP2/6-311G*//HF/6-311G* + 0.9 ZPVE) are in kJ/mol relative to the appropriate minimum geometry. [b] The symbol → indicates that the symmetry of the structure changed during the optimization.

symmetries). These structures (depicted in Figure 1) were then used to obtain single-point UMP2 energies. Calculated structural parameters for **3** are compared with experimentally determined values for **3′** in Figure 3. The energies, zero-point vibrational energies (ZPVE), and number of imaginary frequencies for singlet and

Table 2. Selected Structural Parameters from HF/6-311G* Optimized Geometries of Cyclic Cations[a]

	3 s C_2	**3** t C_2	**3** t C_1	**3** t $C_s \rightarrow C_{2v}$[b]		**3** s C_2	**3** t C_2	**3** t C_1	**3** t $C_s \rightarrow C_{2v}$[b]
P(1)−N(2)	1.598	1.749	1.660	1.747	N(3)−C(7)	1.478	1.450	1.452	1.449
P(1)−N(3)	1.598	1.749	1.891	1.747	C(6)−C(7)	1.542	1.524	1.529	1.525
N(2)−C(6)	1.478	1.450	1.456	1.449	N(2)−P(1)−N(3)	94.1	83.9	84.1	83.9
	7 s C_2	**7** t C_2	**7** t C_1	**7** t $C_s \rightarrow C_{2v}$[b]		**7** s C_2	**7** t C_2	**7** t C_1	**7** t $C_s \rightarrow C_{2v}$[b]
As(1)−N(2)	1.725	1.883	2.046	1.880	N(3)−C(7)	1.476	1.449	1.455	1.447
As(1)−N(3)	1.725	1.883	1.783	1.880	C(6)−C(7)	1.536	1.526	1.530	1.528
N(2)−C(6)	1.476	1.449	1.452	1.447	N(2)−As(1)−N(3)	89.6	80.2	80.3	80.2

4 C_1		**8** C_1		**4** C_1		**8** C_1	
P(1)−N(2)	1.632	As(1)−N(2)	1.768	C(13)−C(15)	1.512	C(13)−C(15)	1.512
P(1)−N(3)	1.630	As(1)−N(3)	1.768	C(14)−C(15)	1.321	C(14)−C(15)	1.322
P(1)−C(12)	1.819	As(1)−C(12)	1.932	N(2)−P(1)−N(3)	94.8	N(2)−As(1)−N(3)	91.8
P(1)−C(13)	1.818	As(1)−C(13)	1.932	N(2)−P(1)−C(12)	113.6	N(2)−As(1)−C(12)	115.3
N(2)−C(6)	1.473	N(2)−C(6)	1.475	N(2)−P(1)−C(13)	117.7	N(2)−As(1)−C(13)	120.9
N(3)−C(7)	1.474	N(3)−C(7)	1.475	N(3)−P(1)−C(12)	120.0	N(3)−As(1)−C(12)	120.8
C(6)−C(7)	1.530	C(6)−C(7)	1.526	N(3)−P(1)−C(13)	115.6	N(3)−As(1)−C(13)	115.3
C(12)−C(14)	1.513	C(12)−C(14)	1.512	C(12)−P(1)−C(13)	96.9	C(12)−As(1)−C(13)	95.0

5 C_1		**9** C_1		**5** C_1		**9** C_1	
P(1)−N(2)	1.872	As(1)−N(2)	2.051	C(13)−C(15)	1.318	C(13)−C(15)	1.321
P(1)−N(3)	1.662	As(1)−N(3)	1.807	C(14)−C(15)	1.502	C(14)−C(15)	1.506
P(1)−C(12)	1.839	As(1)−C(12)	1.960	N(2)−P(1)−N(3)	88.7	N(2)−As(1)−N(3)	87.3
N(2)−C(6)	1.500	N(2)−C(6)	1.497	N(2)−P(1)−C(12)	94.4	N(2)−As(1)−C(12)	92.4
N(2)−C(14)	1.496	N(2)−C(14)	1.506	N(3)−P(1)−C(12)	104.1	N(3)−As(1)−C(12)	103.1
N(3)−C(7)	1.463	N(3)−C(7)	1.457	P(1)−N(2)−C(14)	116.0	As(1)−N(2)−C(14)	116.1
C(6)−C(7)	1.544	C(6)−C(7)	1.530	C(6)−N(2)−C(14)	115.1	C(6)−N(2)−C(14)	112.7
C(12)−C(13)	1.509	C(12)−C(13)	1.506				

6 C_i		**10** C_i		**6** C_i		**10** C_i	
P(1)−N(2)	1.818	As(1)−N(2)	1.940	C(12)−C(14)	1.525	C(12)−C(14)	1.524
P(1)−N(4)	1.925	As(1)−N(4)	2.070	N(2)−P(1)−N(4)	80.6	N(2)−As(1)−N(4)	79.7
P(1)−N(5)	1.614	As(1)−N(5)	1.741	N(2)−P(1)−N(5)	90.6	N(2)−As(1)−N(5)	86.6
N(2)−C(11)	1.517	N(2)−C(11)	1.509	N(4)−P(1)−N(5)	104.7	N(4)−As(1)−N(5)	101.8
N(5)−C(13)	1.471	N(5)−C(13)	1.468	P(1)−N(2)−P(3)	99.4	As(1)−N(2)−As(3)	100.3
C(11)−C(13)	1.525	C(11)−C(13)	1.524				

11 C_s		**12** C_i		**11** C_s		**12** C_i	
As(1)−N(2)	1.724	As(1)−N(2)	1.930			C(11)−C(15)	1.522
N(2)−C(6)	1.476	As(1)−N(4)	2.086			C(13)−C(15)	1.520
C(6)−C(8)	1.522	As(1)−N(5)	1.737			N(2)−As(1)−N(4)	79.5
N(2)−As(1)−N(3)	99.8	N(2)−C(11)	1.513			N(2)−As(1)−N(5)	97.9
		N(5)−C(13)	1.482			N(4)−As(1)−N(5)	104.7
		N(6)−C(14)	1.482			As(1)−N(2)−As(3)	100.5

[a] All lengths are in angstroms; all angles are in degrees. Full listings are available in the Supporting Information. See Chart 1 for structures. [b] The symbol → indicates that the symmetry of the structure changed during the optimization.

triplet cations **3** and **7** are listed in Table 1,[66] and selected structural parameters are listed in Table 2.[66]

The singlet states of the phospholanium (**3**) and arsolanium (**7**) cations are lower in energy than the corresponding triplet states by 308 and 249 kJ/mol, respectively, in qualitative agreement with previous quantum-chemical investigations of structurally simpler pnictogenium cations.[6,30,32,35,37] The singlet−triplet splittings ($E_{s\rightarrow t}$) are much larger than those calculated for $[PH_2]^+$ (68.2, 81.6, and 56.9 kJ/mol[32] and 67.4 kJ/mol[30]) and $[AsH_2]^+$ (87.9, 111.3, and 86.6 kJ/mol[32]). Nevertheless, the splitting in **3** is consistent with those calculated for $[HPF]^+$ (178.2 kJ/mol), $[PF_2]^+$ (351.5 kJ/mol),[30] and $[PBr_2]^+$ (159.20 kJ/mol),[37] just as the splitting in **7** is consistent with those for $[AsCl_2]^+$ (229.7 kJ/mol) and $[AsBr_2]^+$ (183.3 kJ/mol).[35] These similarities are probably due to the π-donor substituents in **3**, **7**, $[HPF]^+$, and $[PF_2]^+$ (and to a lesser extent in the systems with the weaker π-donors Cl and Br), which therefore stabilize the singlet state, with respect to the triplet state, by π-donation.[32,39] The inclusion of the pnictogen center in a five-membered ring imposes an acute N−Pn−N bond angle which is also predicted to stabilize the singlet state relative to the triplet state for carbenes,[40] although the optimized structures for the triplet states of **3** and **7** have even more acute N−Pn−N angles than do the singlets. To assess the relationship between N−Pn−N angle and the relative stability of pnictogenium cations, the energies of a series of simple acyclic pnictogenium cations $[H_2N{-}Pn{-}NH_2]$ (**14**, Pn = P; **15**, Pn = As) were studied on the C_{2v} energy hypersurface. The lowest singlet and triplet states were optimized with no constraints; the resultant structures are shown in Figure 2, and selected structural parameters are

(39) Cramer, C. J.; Dulles, F. J. *J. Am. Chem. Soc.* **1994**, *116*, 9787−9788.

(40) Baird, N. C.; Taylor, K. F. *J. Am. Chem. Soc.* **1978**, *100*, 1333−1338.

Table 3. Selected Structural Parameters from HF/6-311G* Optimized Geometries of Acyclic Species[a]

	14 s C_{2v}	**14** t C_{2v}	**15** s C_{2v}	**15** t C_{2v}		**14** s C_{2v}	**14** t C_{2v}	**15** s C_{2v}	**15** t C_{2v}
Pn(1)−N(2)	1.597	1.753	1.724	1.889	N(2)−Pn(1)−N(3)	104.809	90.047	101.360	87.484
N(2)−H(4)	1.000	1.002	0.998	1.002	Pn(1)−N(2)−H(4)	127.281	127.940	126.233	127.478
N(2)−H(5)	1.000	1.004	0.998	1.004	Pn(1)−N(2)−H(5)	119.003	119.129	119.757	120.168

	14 t C_{2v} MP2	**15** t C_{2v} MP2		**14** t C_{2v} MP2	**15** t C_{2v} MP2
P(1)−N(2)	1.753	1.879	N(2)−P(1)−N(3)	89.136	86.255
N(2)−H(4)	1.015	1.015	P(1)−N(2)−H(4)	126.934	125.990
N(2)−H(5)	1.017	1.017	P(1)−N(2)−H(5)	119.650	120.832

	16 s C_{3v}	**16** s D_{3h}	**16** t D_{3h}	**19** d D_{3h}		**16** s C_{3v}	**16** s D_{3h}	**16** t D_{3h}	**19** d D_{3h}
N−H	0.999	0.985	1.064	1.008	H−N−H	107.4	120.0	120.0	120.0

	17 s C_s	**17** t C_s #1	**17** t C_s #2	**17** t C_1		**17** s C_s	**17** t C_s #1	**17** t C_s #2	**17** t C_1
P(1)−N(2)	1.583	1.617	1.813	1.640	P(1)−N(2)−H(4)	120.7	122.6	122.8	120.7
P(1)−H(3)	1.400	1.389	1.404	1.403	P(1)−N(2)−H(5)	125.7	121.5	122.8	120.7
N(2)−H(4)	1.002	0.998	1.008	1.003	H(4)−N(2)−H(5)	113.6	115.9	113.9	113.5
N(2)−H(5)	1.000	1.000	1.008	1.003	H(3)−P(1)−N(2)−H(4)	180.0	180.0	−94.1	103.5
N(2)−P(1)−H(3)	97.0	117.8	91.1	111.5	H(3)−P(1)−N(2)−H(5)	0.0	0.0	94.1	−103.5

	17 t C_{2v}	**20** d C_1	**20** d C_s #1	**20** d C_s #2		**17** t C_{2v}	**20** d C_1	**20** d C_s #1	**20** d C_s #2
P(1)−N(2)	1.581	1.694	1.685	1.719	P(1)−N(2)−H(4)	123.4	117.7	120.4	115.6
P(1)−H(3)	3.947	1.408	1.408	1.425	P(1)−N(2)−H(5)	123.4	121.7	124.7	115.6
N(2)−H(4)	1.005	0.993	0.991	0.998	H(4)−N(2)−H(5)	113.3	112.8	114.9	109.1
N(2)−H(5)	1.005	0.993	0.991	0.998	H(3)−P(1)−N(2)−H(4)	0.0	−170.6	180.0	−64.6
N(2)−P(1)−H(3)	180.0	95.8	95.8	101.9	H(3)−P(1)−N(2)−H(5)	0.0	−23.5	0.0	64.6

	20 d C_{2v}		**20** d C_{2v}
P(1)−N(2)	4.500	P(1)−N(2)−H(4)	127.5
P(1)−H(3)	1.415	P(1)−N(2)−H(5)	127.5
N(2)−H(4)	1.009	H(4)−N(2)−H(5)	105.0
N(2)−H(5)	1.009	H(3)−P(1)−N(2)−H(4)	0.0
N(2)−P(1)−H(3)	180.0	H(3)−P(1)−N(2)−H(5)	0.0

	18 s C_s	**18** t C_s #1	**18** t C_s #2	**18** t C_s #3		**18** s C_s	**18** t C_s #1	**18** t C_s #2	**18** t C_s #3
As(1)−N(2)	1.709	1.742	2.000	2.000	As(1)−N(2)−H(4)	121.1	122.2	123.5	123.5
As(1)−H(3)	1.515	1.497	1.516	1.516	As(1)−N(2)−H(5)	124.9	120.8	123.5	123.5
N(2)−H(4)	1.000	0.997	1.008	1.008	H(4)−N(2)−H(5)	114.0	117.1	112.9	112.9
N(2)−H(5)	1.000	1.000	1.008	1.008	H(3)−As(1)−N(2)−H(4)	180.0	180.0	−91.9	91.9
N(2)−As(1)−H(3)	95.3	117.6	88.5	88.5	H(3)−As(1)−N(2)−H(5)	0.0	0.0	91.9	−91.9

	18 t C_1	**18** t C_{2v}	**21** d C_1	**21** d C_s #1		**18** t C_1	**18** t C_{2v}	**21** d C_1	**21** d C_s #1
As(1)−N(2)	2.000	1.748	1.830	1.809	As(1)−N(2)−H(4)	123.4	119.3	114.9	120.9
As(1)−H(3)	1.516	1.493	1.521	1.520	As(1)−N(2)−H(5)	123.5	119.3	117.6	124.1
N(2)−H(4)	1.008	0.996	0.996	0.992	H(4)−N(2)−H(5)	113.0	121.5	110.6	115.0
N(2)−H(5)	1.008	0.996	0.995	0.991	H(3)−As(1)−N(2)−H(4)	92.0	0.0	−163.8	180.0
N(2)−As(1)−H(3)	88.5	180.0	94.5	94.4	H(3)−As(1)−N(2)−H(5)	−91.9	0.0	−31.0	0.0

	21 d C_s #2	**21** d C_s #3	**21** d C_{2v}		**21** d C_s #2	**21** d C_s #3	**21** d C_{2v}
As(1)−N(2)	2.056	1.854	1.771	As(1)−N(2)−H(4)	123.8	112.8	119.6
As(1)−H(3)	1.526	1.538	1.452	As(1)−N(2)−H(5)	123.8	112.8	119.6
N(2)−H(4)	1.003	1.000	0.988	H(4)−N(2)−H(5)	112.3	107.9	120.8
N(2)−H(5)	1.003	1.000	0.988	H(3)−As(1)−N(2)−H(4)	−92.1	61.3	0.0
N(2)−As(1)−H(3)	86.4	100.1	180.0	H(3)−As(1)−N(2)−H(5)	92.1	−61.3	0.0

[a] All lengths in are angstroms; all angles are in degrees. Full listings are available in the Supporting Information. See Chart 1 for structures.

listed in Table 3.[66] The calculated energies (Tables 6 and 7, fully optimized structures are assigned a relative energy of 0.0) show that the singlet species is substantially favored in each case ($E_{s\rightarrow t}$: **14**, 395.8 kJ/mol; **15**, 325.2 kJ/mol). The triplet species are optimized with more acute N−Pn−N angles for both phosphenium (104.8 vs 90.0°) and arsenium cations (101.4 vs 87.5°); however, both triplet cations are not true minima (two imaginary frequencies for both P and As). In addition, the effect of the N−Pn−N bond angle on the energy of the cations on the C_{2v} singlet and triplet surfaces was examined by fixing the bond angle and allowing all other parameters to optimize. The results of these calculations are listed in Tables 6 and 7[66] and show that there exists only one minimum for each singlet cation and two "minima" for each of the triplet surfaces. Frequency analysis of each stationary point reveals that the only true minima (N(imag) = 0) on the triplet surface of **14** are at 140 and 150°, which are each more than 100 kJ/mol higher in energy than the lowest energy structure on the C_{2v} surface. There are no true minima on the triplet C_{2v} surface for **15**. Full MP2/6-311G* optimizations for both [$(H_2N)_2$Pn] triplet cations yield results nearly identical with those of the HF/6-311G* optimizations; thus, the inclusion of electron correlation does not predict that C_{2v} triplet cations are stable minima or

Chart 1

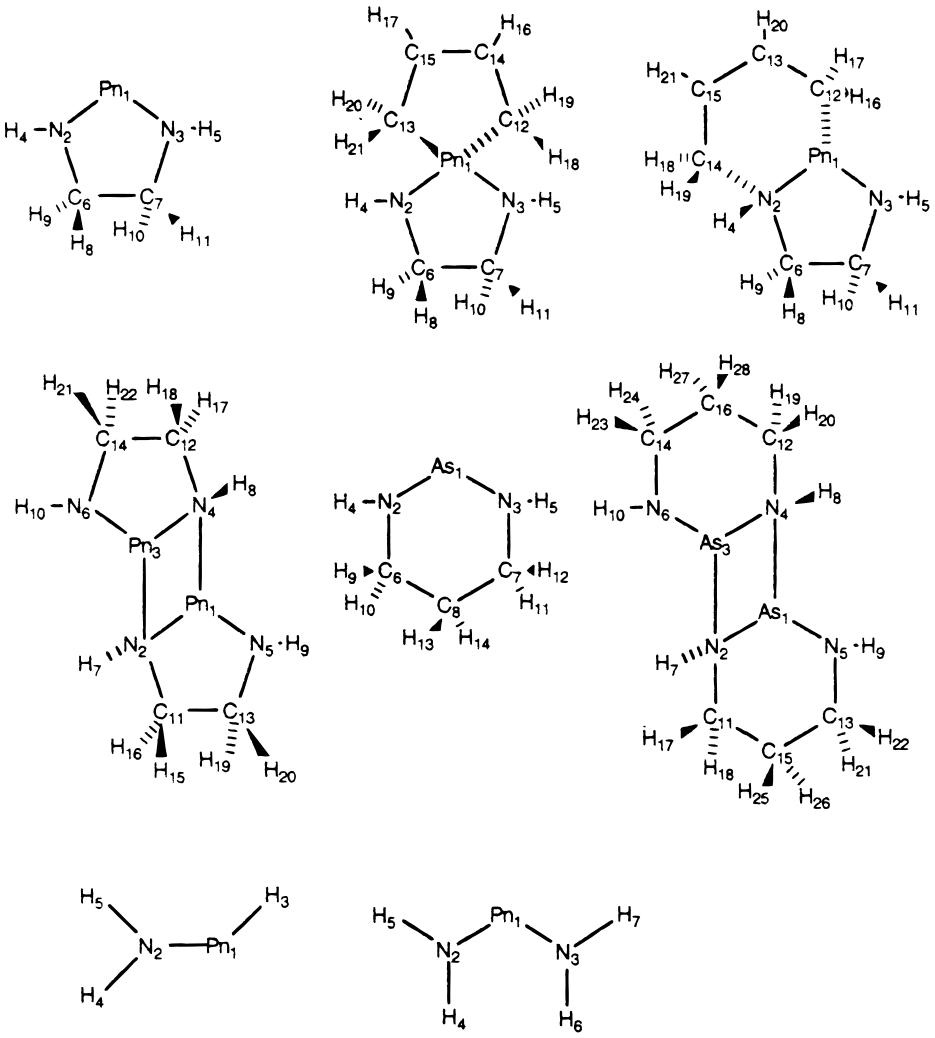

alter the conclusions drawn from the HF calculations. For the cyclic triplet cations **3** and **7**, the decrease in N−Pn−N angle may be explained by the partial filling of the π^* heteroallylic (N−Pn−N) antibonding orbital (*vide infra*).

The Mulliken and NBO charges listed in Table 4 show a concentration of positive charge at the pnictogen center and a localization of negative charge on the N atoms in both systems. The experimentally observed stability may be due to the internal Coulombic stabilization of the "negative−positive−negative" charge distribution for the N−Pn−N fragment (Pn = P, As), consistent with the conclusions of Wiberg based on an *ab initio* study of allylic systems.[41] This phenomenon is likely due to the σ-electronegative stabilizing (and π-donating) effect of an atom such as N, and in this context the vast majority of isolable pnictogenium systems have two nitrogen atoms adjacent to the pnictogen atom.[42]

In contrast to the previous reports,[30,32,35,37] the HF-optimized minima for the triplet states of **3** and **7** (N(imag) = 0) have C_1 symmetry and consist of a partial N−Pn multiple bond (three-electron bond; Pn = P, As) and a nitrogen-based radical. However, at the MP2 level, the C_1 geometry is higher in energy than both the C_2 (N(imag) = 1; $E_{s\rightarrow t}$(MP2) = 288 kJ/mol) and C_s (optimizes to C_{2v}; N(imag) = 2; $E_{s\rightarrow t}$(MP2) = 290 kJ/mol) structures. This indicates that the HF and MP2 energy hypersurfaces are not parallel in the case of the triplet species, which is likely a consequence of the introduction of electron correlation in MP2 calculations. As expected, the singlet species are not as susceptible to the effects of electron correlation, as is evident from the optimization of **3** at the full MP2/6-311G* level of theory, which yields a structure and energy (6.85 kJ/mol lower) nearly identical with those of **3** at MP2/6-311G*//HF/6-311G* optimization.

The charge and spin distributions shown in Tables 4 and 5, respectively, are similar for triplets **3** and **7** (C_1 symmetry; N(imag) = 0) with positive charge localized on the pnictogen atom and negative charge on the nitrogen atoms. The charge on the pnictogen center is significantly lower for the triplet than for the singlet in each case (**3** singlet, 1.12; triplet, 0.77; **7** singlet, 1.16; triplet, 0.82) and the negative charges on the nitrogen atoms are no longer equal (**3** triplet N, −0.86 and −0.50; **7** triplet N, −0.50 and −0.87). The spin densities are also found almost exclusively in the N−Pn−N moieties which, along with structural parameters and NBO

(41) Wiberg, K. B.; Breneman, C. M.; LePage, T. J. *J. Am. Chem. Soc.* **1990**, *112*, 61−72.
(42) Reed, R. W.; Xie, Z.; Reed, C. A. *Organometallics* **1995**, *14*, 5002−5004 and references therein.

Table 4. Mulliken and Natural Bond Orbital (NBO) Charge Distributions of Selected Atoms[a]

	3 s C_2		**3** t C_1			**3** s C_2		**3** t C_1	
	Mulliken	NBO	Mulliken	NBO		Mulliken	NBO	Mulliken	NBO
P(1)	1.123	1.552	0.772	0.968	H(4)	0.450	0.439	0.446	0.429
N(2)	−0.877	−1.003	−0.865	−0.978	H(5)	0.450	0.439	0.450	0.397
N(3)	−0.877	−1.003	−0.505	−0.370					

	3 t C_2		**3** t $C_s \rightarrow C_{2v}$[b]			**3** t C_2		**3** t $C_s \rightarrow C_{2v}$[b]	
	Mulliken	NBO	Mulliken	NBO		Mulliken	NBO	Mulliken	NBO
P(1)	0.627	0.786	0.620	0.786	H(4)	0.450	0.417	0.448	0.416
N(2)	−0.625	−0.599	−0.625	−0.599	H(5)	0.450	0.417	0.448	0.416
N(3)	−0.625	−0.599	−0.625	−0.599					

	4 C_1		**5** C_1			**4** C_1		**5** C_1	
	Mulliken	NBO	Mulliken	NBO		Mulliken	NBO	Mulliken	NBO
P(1)	1.610	2.049	0.940	1.273	H(5)	0.423	0.422	0.423	0.410
N(2)	−0.928	−1.036	−0.804	−0.699	C(12)	−0.796	−0.705	−0.791	−0.718
N(3)	−0.931	−1.036	−0.902	−1.022	C(13)	−0.792	−0.706	−0.142	−0.141
H(4)	0.425	0.422	0.447	0.412					

	6 C_i			**6** C_i	
	Mulliken	NBO		Mulliken	NBO
P(1)	1.190	1.532	H(7)	0.487	0.451
N(2)	−1.033	−1.030	H(9)	0.471	0.454
N(5)	−0.898	−1.038			

	7 s C_2		**7** t C_1			**7** s C_2		**7** t C_1	
	Mulliken	NBO	Mulliken	NBO		Mulliken	NBO	Mulliken	NBO
As(A)	1.161	1.642	0.824	1.082	H(4)	0.439	0.429	0.439	0.386
N(2)	−0.868	−1.031	−0.498	−0.394	H(5)	0.439	0.429	0.434	0.422
N(3)	−0.868	−1.031	−0.872	−1.028					

	7 t C_2		**7** t $C_s \rightarrow C_{2v}$*			**7** t C_2		**7** t $C_s \rightarrow C_{2v}$*	
	Mulliken	NBO	Mulliken	NBO		Mulliken	NBO	Mulliken	NBO
As(1)	0.650	0.853	0.647	0.851	H(4)	0.440	0.407	0.438	0.407
N(2)	−0.618	−0.613	−0.621	−0.612	H(5)	0.440	0.407	0.438	0.407
N(3)	−0.618	−0.613	−0.621	−0.612					

	8 C_1		**9** C_1			**8** C_1		**9** C_1	
	Mulliken	NBO	Mulliken	NBO		Mulliken	NBO	Mulliken	NBO
As(1)	1.571	2.055	0.997	1.354	H(5)	0.404	0.407	0.395	0.387
N(2)	−0.887	−1.020	−0.802	−0.722	C(12)	−0.753	−0.691	−0.769	−0.723
N(3)	−0.887	−1.020	−0.845	−1.018	C(13)	−0.753	−0.691	−0.154	−0.126
H(4)	0.404	0.407	0.443	0.410					

	10 C_i			**12** C_i			**10** C_i			**12** C_i	
	Mulliken	NBO		Mulliken	NBO		Mulliken	NBO		Mulliken	NBO
As(1)	1.272	1.656	As(1)	1.271	1.652	H(7)	0.468	0.438	H(7)	0.459	0.430
N(2)	−1.026	−1.074	N(2)	−1.039	−1.077	H(9)	0.458	0.444	H(9)	0.440	0.426
N(5)	−0.914	−1.067	N(5)	−0.950	−1.078						

	11 C_s			**11** C_s	
	Mulliken	NBO		Mulliken	NBO
As(1)	1.155	1.623	H(4)	0.434	0.420
N(2)	−0.885	−1.034			

	3 prep C_1		**7** prep C_1		**11** prep C_1			**3** prep C_1		**7** prep C_1		**11** prep C_1	
	Mulliken	NBO	Mulliken	NBO	Mulliken	NBO		Mulliken	NBO	Mulliken	NBO	Mulliken	NBO
1 P	1.149	1.526	1.133	1.603	1.133	1.602	4 H	0.420	0.404	0.405	0.395	0.399	0.389
2 N	−0.866	−0.968	−0.802	−0.980	−0.813	−0.992	5 H	0.458	0.442	0.444	0.432	0.431	0.416
3 N	−0.850	−0.979	−0.842	−1.008	−0.863	−1.016							

	14 s C_{2v}		**14** t C_{2v}			**14** s C_{2v}		**14** t C_{2v}	
	Mulliken	NBO	Mulliken	NBO		Mulliken	NBO	Mulliken	NBO
P(1)	1.162	1.568	0.660	0.792	H(4)	0.446	0.431	0.439	0.398
N(2)	−0.995	−1.153	−0.735	−0.706	H(5)	0.467	0.438	0.466	0.412

Table 4. (Continued)

	15 s C_{2v}		**15** t C_{2v}			**15** s C_{2v}		**15** t C_{2v}	
	Mulliken	NBO	Mulliken	NBO		Mulliken	NBO	Mulliken	NBO
As(1)	1.249	1.673	0.704	0.857	H(4)	0.440	0.423	0.435	0.390
N(2)	−1.017	−1.188	−0.741	−0.720	H(5)	0.453	0.428	0.454	0.402
	16 s C_{3v}		**16** s D_{3h}			**16** s C_{3v}		**16** s D_{3h}	
	Mulliken	NBO	Mulliken	NBO		Mulliken	NBO	Mulliken	NBO
N(1)	−1.022	−0.983	−1.090	−1.069	H(2)	0.341	0.328	0.363	0.356
	16 t D_{3h}		**19** d D_{3h}			**16** t D_{3h}		**19** d D_{3h}	
	Mulliken	NBO	Mulliken	NBO		Mulliken	NBO	Mulliken	NBO
N(1)	−0.236	−0.408	−0.478	−0.231	H(2)	0.079	0.136	0.493	0.410
	17 s C_s		**17** t C_1			**17** s C_s		**17** t C_1	
	Mulliken	NBO	Mulliken	NBO		Mulliken	NBO	Mulliken	NBO
P(1)	0.861	1.266	0.700	1.082	H(4)	0.473	0.441	0.476	0.438
N(2)	−0.906	−1.066	−0.853	−0.977	H(5)	0.473	0.444	0.476	0.438
H(3)	0.099	−0.085	0.202	0.019					
	17 t C_s #1		**17** t C_s #2			**17** t C_s #1		**17** t C_s #2	
	Mulliken	NBO	Mulliken	NBO		Mulliken	NBO	Mulliken	NBO
P(1)	0.796	1.238	0.534	0.758	H(4)	0.478	0.450	0.477	0.407
N(2)	−0.986	−1.169	−0.610	−0.510	H(5)	0.479	0.450	0.477	0.407
H(3)	0.233	0.030	0.122	−0.061					
	17 t C_{2v}		**20** d C_1			**17** t C_{2v}		**20** d C_1	
	Mulliken	NBO	Mulliken	NBO		Mulliken	NBO	Mulliken	NBO
P(1)	0.940	1.230	0.276	0.529	H(4)	0.479	0.448	0.380	0.369
N(2)	−0.902	−1.127	−1.025	−1.140	H(5)	0.479	0.448	0.381	0.370
H(3)	0.005	0.001	−0.012	−0.129					
	20 d C_s #1		**20** d C_s #2			**20** d C_s #1		**20** d C_s #2	
	Mulliken	NBO	Mulliken	NBO		Mulliken	NBO	Mulliken	NBO
P(1)	0.276	0.525	0.341	0.631	H(4)	0.385	0.375	0.370	0.359
N(2)	−1.036	−1.149	−1.039	−1.173	H(5)	0.387	0.376	0.370	0.359
H(3)	−0.013	−0.128	−0.041	−0.176					

	20 d C_{2v}			**20** d C_{2v}	
	Mulliken	NBO		Mulliken	NBO
P(1)	−0.006	0.167	H(4)	0.312	0.255
N(2)	−0.617	−0.509	H(5)	0.312	0.255
H(3)	−0.001	−0.168			

	18 s C_s		**18** t C_1			**18** s C_s		**18** t C_1	
	Mulliken	NBO	Mulliken	NBO		Mulliken	NBO	Mulliken	NBO
As(1)	0.888	1.345	0.553	0.819	H(4)	0.462	0.432	0.463	0.390
N(2)	−0.945	−1.111	−0.614	−0.507	H(5)	0.465	0.435	0.463	0.390
H(3)	0.130	−0.101	0.136	−0.091					
	18 t C_s #1		**18** t C_s #2			**18** t C_s #1		**18** t C_s #2	
	Mulliken	NBO	Mulliken	NBO		Mulliken	NBO	Mulliken	NBO
As(1)	0.813	1.260	0.553	0.819	H(4)	0.467	0.440	0.463	0.389
N(2)	−1.000	−1.178	−0.614	−0.507	H(5)	0.466	0.441	0.463	0.389
H(3)	0.255	0.037	0.136	−0.091					
	18 t C_s #3		**18** t C_{2v}			**18** t C_s #3		**18** t C_{2v}	
	Mulliken	NBO	Mulliken	NBO		Mulliken	NBO	Mulliken	NBO
As(1)	0.553	0.819	0.598	0.962	H(4)	0.462	0.389	0.473	0.443
N(2)	−0.614	−0.507	−0.927	−1.082	H(5)	0.462	0.389	0.473	0.443
H(3)	0.136	−0.091	0.383	0.234					
	21 d C_1		**21** d C_s #1			**21** d C_1		**21** d C_s #1	
	Mulliken	NBO	Mulliken	NBO		Mulliken	NBO	Mulliken	NBO
As(1)	0.290	0.586	0.302	0.587	H(4)	0.364	0.359	0.377	0.370
N(2)	−1.031	−1.160	−1.065	−1.186	H(5)	0.370	0.362	0.383	0.373
H(3)	0.006	−0.146	0.003	−0.145					

Table 4. (Continued)

	21 d C_s #2		**21** d C_s #3			**21** d C_s #2		**21** d C_s #3	
	Mulliken	NBO	Mulliken	NBO		Mulliken	NBO	Mulliken	NBO
As(1)	−0.188	−0.101	0.337	0.658	H(4)	0.398	0.334	0.360	0.352
N(2)	−0.616	−0.457	−1.032	−1.175	H(5)	0.398	0.334	0.360	0.352
H(3)	0.009	−0.109	−0.025	−0.186					

	21 d C_{2v}			**21** d C_{2v}	
	Mulliken	NBO		Mulliken	NBO
As(1)	−0.200	0.057	H(4)	0.411	0.387
N(2)	−0.935	−1.032	H(5)	0.411	0.387
H(3)	0.313	0.201			

[a] Full listings are available in the Supporting Information. See Chart 1 for structures. [b] The symbol → indicates that the symmetry of the structure changed during the optimization.

Table 5. Calculated Spin Densities of Doublet and Triplet Species of Selected Atoms[a]

	3 t C_1	**3** t C_2	**3** t C_s → C_{2v}
P(1)	0.787 359	0.570 222	0.567 805
N(2)	0.234 2	0.797 118	0.798 349
N(3)	1.111 636	0.797 118	0.798 349

	7 t C_1	**7** t C_2	**7** t C_s → C_{2v}
As(1)	0.771 37	0.457 429	0.457 074
N(2)	1.139 47	0.855 826	0.855 291
N(3)	0.215 669	0.855 826	0.855 291

	14 t C_{2v}	**14** t C_{2v} MP2	**15** t C_{2v}
Pn(1)	0.569 402	0.573 133	0.455 039
N(2)	0.829 083	0.829 303	0.885 66
H(4)	−0.056 652	−0.057 781	−0.056 115
H(5)	−0.057 132	−0.058 088	−0.057 065

	17 t C_1	**17** t C_s #1	**17** t C_s #2	**17** t C_{2v}
P(1)	1.459 99	1.738 679	1.014 774	1.184 236
N(2)	0.421 357	0.210 809	1.068 443	−0.256 47
H(3)	0.145 637	0.067 874	0.020 893	0.995 796
H(4)	−0.013 494	−0.023 644	−0.052 055	0.038 219
H(5)	−0.013 49	0.006 282	−0.052 055	0.038 219

	20 d C_1	**20** d C_s #1	**20** d C_s #2	**20** d C_{2v}
P(1)	0.964 238	0.949 062	1.092 082	2.092 449
N(2)	0.116 866	0.141 537	−0.063 631	−1.144 654
H(3)	−0.054 573	−0.053 942	−0.056 067	−0.090 582
H(4)	−0.014 537	−0.018 096	0.013 808	0.071 393
H(5)	−0.011 994	−0.018 562	0.013 808	0.071 393

	18 t C_1	**18** t C_s #1	**18** t C_s #2	**18** t C_s #3	**18** t C_{2v}
As(1)	0.976 501	1.654 095	0.976 405	0.976 396	2.205 972
N(2)	1.140 386	0.241 983	1.140 418	1.140 591	0.058 054
H(3)	−0.000 567	0.120 56	−0.000 519	−0.000 64	−0.267 776
H(4)	−0.058 171	−0.024 501	−0.058 152	−0.058 174	0.001 875
H(5)	−0.058 15	0.007 862	−0.058 152	−0.058 174	0.001 875

	21 d C_1	**21** d C_s #1	**21** d C_s #2	**21** d C_s #3	**21** d C_{2v}
As(1)	0.983 212	0.947 211	−0.084 1	1.095 731	1.101254
N(2)	0.087 019	0.137 583	1.156 323	−0.058 375	0.089 37
H(3)	−0.055 764	−0.054 055	0.064 992	−0.056 85	−0.168 619
H(4)	−0.008 674	−0.015 264	−0.068 607	0.009 747	−0.011 002
H(5)	−0.005 794	−0.015 475	−0.068 607	0.009 747	−0.011 002

	16 t D_{3h}	**19** d D_{3h}
N(1)	0.917 497	1.202 094
H(2)	0.360 834	−0.067 365

[a] Full listing are available in the Supporting Information. See Chart 1 for structures. [b] The symbol → indicates that the symmetry of the structure changed during the optimization.

analysis, suggest that the triplets each contain a Pn−N multiply bonded (three-electron bond) radical (sum of spin densities on Pn and N: **3**, 1.01; **7**, 0.98) cation and a separated nitrogen radical (spin density: **3**, 1.11; **7**, 1.13).

In an attempt to understand the unexpected symmetry and bonding of triplets **3** and **7**, calculations were performed on the singlet and triplet ground states of NH_3 (**16**), $[H_2NPH]^+$ (**17**),[31] $[H_2NAsH]^+$ and (**18**) and the doublet ground states of $[NH_3]^{\bullet+}$ (**19**), $[H_2NPH]^{\bullet}$ (**20**),

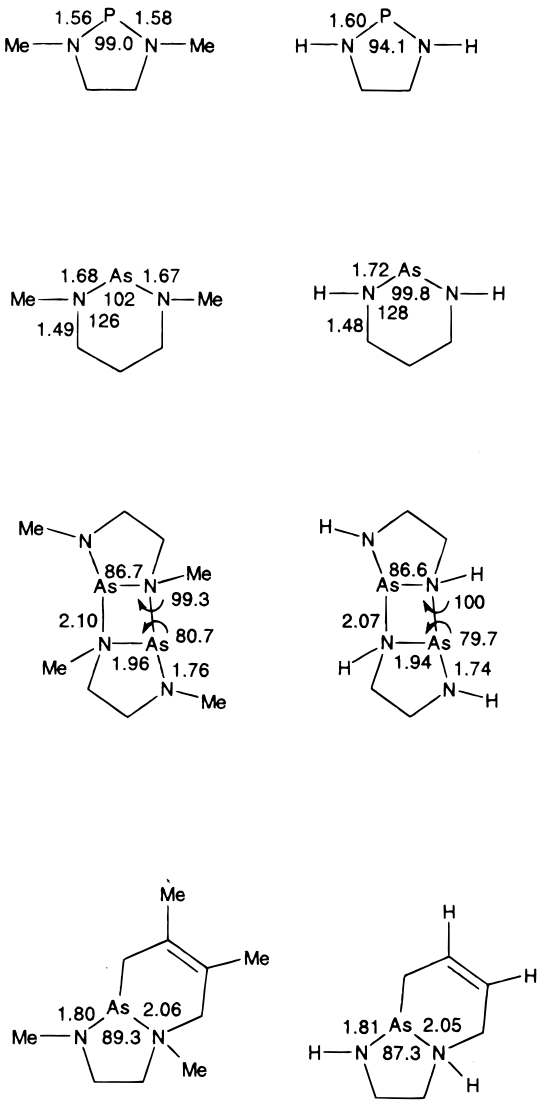

Figure 3. Comparison of selected experimentally (left) and theoretically (right) determined structural parameters for **3**, **11**, **10**, and **9** (angles in deg, lengths in Å).

and $[H_2NAsH]^{\bullet}$ (**21**). All appropriate symmetries were examined for each species, and the energies, the number of imaginary frequencies, and the ZPVEs are listed in Table 1. The structures are shown in Figure 2, and the structural parameters are listed in Table 3. Models **16**−**18** are not consistent with the results obtained for triplets **3** and **7** and predictably confirm that triplet ammonia is much less favorable than singlet ammonia and has a much larger singlet−triplet splitting (511.7 kJ/mol) than both **16** and **17**. An isodesmic comparison of the singlet and triplet species is thus unproductive; however, an isogyric comparison of the doublet species **19**, **20**, and **21** to **16**, **17**, and **18** accurately reproduces the behavior observed in triplets **3** and **7**. The lengths for the shorter Pn−N bond in triplets **3** and **7** are consistent with those of doublets **20** and **21**, respectively (**3** t C_1 N(3)−H(5) bond (1.005 Å) (**7** t C_1 N(2)−H(4) (1.005 Å)) (the hydrogen atom bonded to the nitrogen atom not involved in multiple bonding) is most closely reproduced by the 1.008 Å N−H bond in the ammonium radical cation **19**. The structures of triplet cations **3** and **7** are thus best explained as a combination of distinct radical and radical cation units; however, the reason for the adoption of this structure remains unclear. A possible rationalization is found in the reaction energies shown in Table 8.[66] Isogyric reaction energies show that singlet ammonia and the lowest energy triplet cation are favored over all of the combinations of doublet species; however, if the singlet and triplet species are restricted to the symmetries observed in cations **3** and **7** (planar $R_2N-Pn-NR_2$ moiety) the doublet species are favored (18.6 kJ/mol, Pn = P; 29.0 kJ/mol, Pn = As).

Dimerization of Pnictogenium Cations. Carbenes and their analogues are by definition formally subvalent (dicoordinate) and electron deficient, and as such, they are susceptible to dimerization to enable the adoption of a "normal" coordination number and valence octet. For example, group 14 carbenoids without π-donor substituents (including carbenes with π-donors) dimerize to form olefin-type compounds **22**.[6,43] Certain

22 **23**

heavier carbene analogues bearing π-donor groups are predicted[6,44] and observed[6,45] to form bridged dimers **23**, which may be considered σ-bonded alternatives to the corresponding multiply bonded monomers (two- or four-π-electron systems) or mutual donor−acceptor complexes of the monomers. π-Bonding is weaker for heavier elements ($n > 2$) so that four single bonds (four σ-bonds) are energetically favored over two double bonds (two σ-bonds and two π-bonds), as depicted in Scheme 1. This prediction arises from the assumption that π-overlap decreases as n increases, although Schleyer has shown that it is actually the increase in the energy of planarization with increasing n that decreases the favorability of π-interactions.[46] The experimentally observed dimers of arsolanium cations,[19] in contrast to the universally monomeric structures of phospholanium salts, are consistent with such trends. However, our recent isolation and characterization of the monomeric arsenanium salt **11′**$[GaCl_4]$ implies that the centrosymmetric dimer **10′**$[GaCl_4]_2$ ($P2_1/n$ space group) is likely a

(43) Regitz, M. *Angew. Chem., Int. Ed. Engl.* **1991**, *30*, 674−676 and references therein.

(44) See, for example: (a) Apeloig, Y. In *The Chemistry of Organic Silicon Compounds*; Patai, S., Rappoport, Z., Eds.; Wiley: Toronto, 1989; Part 1, Chapter 2, and references therein. (b) Maxka, J.; Apeloig, Y. *J. Chem. Soc., Chem. Commun.* **1990**, 737−739. (c) Karni, M.; Apeloig, Y. *J. Am. Chem. Soc.* **1990**, *112*, 8589−8590. (d) Apeloig, Y.; Müller, T. *J. Am. Chem. Soc.* **1995**, *117*, 5363−5364.

(45) See, for example: (a) Schönherr, H.-J.; Wanzlick, H.-W. *Chem. Ber.* **1970**, *103*, 1037−1046, and references therein. (b) Veith, M. *Z. Naturforsch., B* **1978**, *33*, 1−6. (c) Veith, M. *Z. Naturforsch., B* **1978**, *33*, 7−13. (d) Veith, M.; Recktenwald, D.; Humpfer, E. *Z. Naturforsch., B* **1978**, *33*, 14−19. (e) Jutzi, P.; Holtmann, U.; Bögge, H.; Müller, A. *J. Chem. Soc., Chem. Commun.* **1988**, 305−306. (f) Sakamoto, K.; Tsutsui, S.; Sakurai, H.; Kira, M. *Bull. Chem. Soc. Jpn.* **1997**, *70*, 253−260.

(46) Schleyer *et al.* have determined that it is not inherently poor π-overlap but an increasing hybridization (planarization) energy that renders heavier π-bonding unfavorable: Kapp, J.; Schade, C.; El-Nahasa, A. M.; Schleyer, P. v. R. *Angew. Chem., Int. Ed. Engl.* **1996**, *35*, 2236−2238.

Table 6. Effect of Changes in N−P−N Angle for C_{2v} Acyclic Phosphenium Cations 14: Computed Energies (HF/6-311G* and MP2/6-311G*//HF/6-311G*) and Zero Point Vibrational Energies for All Calculations[a]

N−P−N angle	*N*(imag)	HF	MP2	ZPVE	rel energy
		14 s C_{2v}			
60	2	−451.514 21	−451.996 58	0.057 46	591.40
70	1	−451.644 74	−452.108 39	0.059 28	302.13
80	1	−451.722 55	−452.175 81	0.059 55	125.75
90	0	−451.762 08	−452.209 90	0.059 53	36.21
100	0	−451.777 23	−452.222 52	0.059 40	2.76
104.8073	0	−451.778 73	−452.223 49	0.059 30	0.00
110	0	−451.777 17	−452.221 74	0.059 22	4.41
120	0	−451.766 64	−452.211 74	0.059 10	30.36
130	0	−451.747 84	−452.194 47	0.058 98	75.41
140	0	−451.721 87	−452.170 92	0.058 80	136.81
150	0	−451.689 34	−452.141 70	0.058 49	212.81
160	0	−451.650 59	−452.107 24	0.057 89	301.87
170	0	−451.605 85	−452.068 36	0.056 35	400.31
		14 t C_{2v}			
60	4	−451.450 81	−451.880 93	0.051 44	484.99
70	3	−451.625 04	−452.043 08	0.054 50	66.51
80	3	−451.657 20	−452.071 69	0.053 33	−11.40
90	2	−451.665 15	−452.078 02	0.065 30	0.28
90.0467	2	−451.665 15	−452.078 02	0.065 18	0.00
100	2	−451.660 06	−452.072 27	0.057 36	−3.38
110	4	−451.645 66	−452.058 67	0.052 95	21.90
120	4	−451.646 92	−452.060 21	0.052 69	17.25
130	4	−451.641 91	−452.056 07	0.052 51	27.69
140	0	−451.581 64	−452.023 05	0.058 05	127.48
150	0	−451.607 61	−452.045 83	0.084 90	131.13
160	1	−451.626 44	−452.062 42	0.056 15	19.62
170	1	−451.637 85	−452.062 42	0.056 34	20.06
		14 t C_{2v}			
89.135	2		−452.078 75	0.183 19[b]	

[a] Absolute energies are in hartrees. *N*(imag) indicates the number of imaginary vibrational frequencies. Relative energies (MP2/6-311G*//HF/6-311G* + 0.9 ZPVE) are in kJ/mol relative to the appropriate optimized minimum geometry. [b] Optimized.

function of crystal packing.[18] Steplike dimeric structures analogous to those of the cation **10′** have been observed in centrosymmetric space groups for compounds involving elements from groups 13,[47] 14,[48] and 15.[18] To further evaluate and quantify the dimerization reaction, the structures of dimers **6** and **10** have been optimized at the HF/6-311G* level with restriction to C_i symmetry (*vide supra*) and are shown in Figure 1. The MP2 energies obtained at these geometries and their ZPVE values are listed with those of the monomers **3** and **7** in Table 1. Dimerization reaction energies are listed in Table 8. Selected calculated structural features are compared with those observed experimentally (X-ray crystallographic studies) in Figure 3.[16,23,19,18] The structures of cations **3′**, **10′**, and **11′** are very closely approximated by the optimized geometries of **3**, **10**, and **11**, respectively. All bond lengths are within the estimated standard deviations obtained experimentally, and all angles are within 5° of the experimentally determined values.

The energy of dimerization for the arsolanium cation **7′** is calculated to be +206.7 kJ/mol, confirming that the monomer is favored in the gas phase in contrast to the experimentally observed solid-state structure **10′**. An experimental observation consistent with the unfavorability of dimerization is found in the case of the six-membered-ring analogue of **7′**[$GaCl_4$]. The arsenanium cation in the salt **11′**[$GaCl_4$] is unquestionably monomeric in the solid state (space group $Pca2_1$): the closest intermolecular As−N contact is 5.62 Å, despite the weak dimer structure observed for the chloroarsine **13** (space group $P2_1/n$).[18] The energy of dimerization of **11** to centrosymmetric dimer **12** is calculated to be +247.9 kJ/mol, almost 20% more than that of **7**, which shows that six-membered cyclic **11** is more stable vis à vis dimerization than is five-membered cyclic **7** and may imply that **11** is an inherently more stable carbenoid environment. A possible explanation for the seemingly enhanced stability of **11** is that the less restricted six-membered ring allows the N−As−N angle (99.8° in **11**) to approach the optimum angle (101.4° in the acyclic analogue, vide supra), whereas the smaller ring constrains the N−As−N angle to be significantly more accute (89.6° in **7**). In acyclic $[(H_2N)As]^+$, changing the angle at the arsenic atom from 100° to 90° results in a destabilization of 17.9 kJ/mol (or 35.8 kJ/mol for the two molecules that form the dimer, *vide infra*), which represents almost the entire difference between the dimerization energies of **7** and **11**.

Similarly, the phosphenium cation in salt **3′**[$GaCl_4$] is monomeric (space group $P2_1$) and the calculated energy of dimerization for **3** (+277.4 kJ/mol) is greater than those for **7** or **11**; however, the rationale for the significant difference in dimerization energies between the phosphenium and arsenium systems is different. The relative stability of the phosphenium cation in comparison to the analogous arsenium species with respect to dimerization is consistent with more favorable N−P (2p−3p)π-bonding versus N−As (2p−4p)π-bonding in the respective monomers.

(47) (a) Brown, D. S.; Decken, A.; Schnee, C. A.; Cowley, A. H. *Inorg. Chem.* **1995**, *34*, 6415−6416. (b) Cowley, A. H.; Brown, D. S.; Decken, A.; Kamepalli, S. *J. Chem. Soc., Chem. Commun.* **1996**, 2425−2426.

(48) Sohn, H.; Powell, D. R.; West, R.; Hong, J.-H.; Joo, W.-C. *Organometallics* **1997**, *16*, 6, 2770−2772.

Table 7. Effect of Changes in N−As−N Angle for C_{2v} Acyclic Arsenium Cations 15: Computed Energies (HF/6-311G* and MP2/6-311G*//HF/6-311G*) and Zero Point Vibrational Energies for All Calculations[a]

N−As−N angle	*N*(imag)	HF	UMP2	ZPVE	rel energy
		15 s C_{2v}			
60	2	−2 344.970 19	−2 345.446 15	0.056 80	452.04
70	2	−2 345.078 29	−2 345.537 62	0.057 31	213.08
80	1	−2 345.137 99	−2 345.588 71	0.057 45	79.26
90	0	−2 345.165 35	−2 345.612 02	0.057 46	18.08
100	0	−2 345.173 49	−2 345.618 72	0.057 32	0.17
101.3561	0	−2 345.173 59	−2 345.618 77	0.057 30	0.00
110	0	−2 345.169 92	−2 345.615 31	0.057 17	8.79
120	0	−2 345.157 99	−2 345.604 71	0.057 03	36.27
130	0	−2 345.139 17	−2 345.588 16	0.056 83	79.24
140	0	−2 345.114 26	−2 345.566 47	0.056 49	135.40
150	0	−2 345.083 83	−2 345.540 27	0.055 91	202.82
160	1	−2 345.048 42	−2 345.510 50	0.054 75	278.24
170	2	−2 345.008 99	−2 345.479 56	0.053 15	355.69
		15 t C_{2v}			
60	3	−2 345.007 68	−2 345.422 52	0.053 07	180.04
70	3	−2 345.061 51	−2 345.473 62	0.052 88	45.46
80	2	−2 345.086 44	−2 345.495 03	0.057 34	−0.22103
87.483	2	−2 345.086 44	−2 345.495 02	0.057 42	0.00
90	2	−2 345.086 44	−2 345.495 02	0.057 42	0.00
100	2	−2 345.086 44	−2 345.495 02	0.057 39	−0.10
110	2	−2 345.086 44	−2 345.495 03	0.057 39	−0.10
120	2	−2 345.086 44	−2 345.495 03	0.057 39	−0.09
130	2	−2 345.086 44	−2 345.495 02	0.057 39	−0.11
140	2	−2 345.086 44	−2 345.495 03	0.057 38	−0.14
150	2	−2 345.086 44	−2 345.495 02	0.057 40	−0.08
160	4	−2 345.045 78	−2 345.459 69	0.051 55	78.88
170	4	−2 345.045 78	−2 345.459 70	0.051 55	78.86
		15 t C_{2v}			
86.2547	n/d		−2 345.495 93	n/d	

[a] Absolute energies are in hartrees. *N*(imag) indicates the number of imaginary vibrational frequencies. Relative energies (MP2/6-311G*//HF/6-311G* + 0.9 ZPVE) are in kJ/mol relative to the appropriate optimized minimum geometry. [b] MP2. [c] Optimized; not determined.

Table 8. Calculated Enthalpies of Reactions, Dimerizations, and Singlet−Triplet Energy Splittings[a]

reacn	MP2	HF
Cycloaddition Reaction Energies		
3 + *trans*−1,3-butadiene → **4**	−163.74	−138.11
3 + *trans*−1,3-butadiene → **5**	−112.20	−61.59
7 + *trans*−1,3-butadiene → **8**	−85.92	−59.23
7 + *trans*−1,3-butadiene → **9**	−144.45	−93.06
Dimerization Energies		
3 + **3** → **6**	277.44	337.27
7 + **7** → **10**	206.70	260.63
11 + **11** → **12**	247.92	294.00
Isogyric Reaction Energies		
16 s + **17** t C_1 → **16** t + **17** s	317.41	320.69
16 s + **17** t C_s #2 → **19** d + **20** d C_1	22.24	22.73
16 s D_{3h} + **17** t C_s #1 → **19** d + **20** d C_1	−18.60	−66.25
16 s + **18** t C_1 → **16** t + **18** s	306.41	382.41
16 s + **18** t C_s #2 → **19** d + **21** d C_1	45.91	61.73
16 s D_{3h} + **18** t C_s #1 → **19** d + **21** d C_1	−29.05	−78.82

[a] All enthalpies in kJ/mol.) MP2 denotes MP2/6-311G*//HF/6-311G* + 0.90 ZPVE; HF denotes HF/6-311G* + 0.90 ZPVE.

Scheme 1

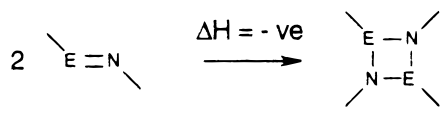

An estimate of the dimerization activation energy was obtained through the use of the generalized transition state method,[49] in which the dimerization process is assumed to proceed via the deformation of each monomeric unit to the structure in which it is found in the dimer followed by the coupling of two of these "protodimeric" moieties (**3** prep, **7** prep and **11** prep in the following discussion). In most systems where dimerizations occur the energy of the deformation of each monomer (the energy of which is denoted ΔE_{prep}) is generally endoenthalpic and the coupling is exoenthalpic. The energy of coupling is divided into two terms: $\Delta E°$ (the energy of the stabilizing electrostatic interactions and the destabilizing repulsive interaction between the two fragments) and ΔE_{el} (the energy of the stabilizing interaction of filled and empty orbitals on each fragment).[50] The dimerization energy can be expressed as

$$\Delta E_{dimerization} = E_{dimer} - 2E_{monomer} \quad (1)$$

and

$$\Delta E_{dimerization} = 2\Delta E_{prep} + \Delta E° + \Delta E_{el} \quad (2)$$

The dimerizations studied in this work are all highly endothermic (*vide supra*), and analysis of the relative contributions to the dimerization energy using eq 2 offers valuable insight into the cause of this endothermicity. In all three systems, the term $\Delta E° + \Delta E_{el}$ is negligible (**3**, 10.4 kJ/mol; **7**, 25.6 kJ/mol; **11**, 3.0 kJ/mol), which is likely because of the repulsion caused by the positive charge on each fragment (destabilizing) and

(49) Ziegler, T.; Rauk, A. *Theor. Chim. Acta* **1977**, *46*, 1−10.

(50) See, for example: Sandblom, N.; Ziegler, T.; Chivers, T. *Inorg. Chem.* **1998**, *37*, 354−359.

the lack of purely filled or empty π-orbitals in the monomeric fragments (some π-delocalization is still present in the monomer fragments in their respective dimer geometries). Thus, the dominant factor contributing to $\Delta E_{\text{dimerization}}$ is ΔE_{prep}, the energy of distorting the monomers from their most stable geometry to the geometry observed in the dimer. The distortion energy is very large for each monomer (ΔE_{prep}: **3**, 133.5 kJ/mol; **7**, 90.6 kJ/mol; **11**, 122.4 kJ/mol) and precludes the formation of the dimers. Note that this distortion energy may also be used as a gauge for the relative stabilities of **7** and **11** in that the six-membered ring containing the more favorable arsenium N−As−N angle requires 35% more energy to distort than does the relatively less stable five-membered ring.

Butadiene Cycloaddition Reactions. Cycloaddition reactions are of immense utility to synthetic chemists,[51] and the theoretical principles that explain pericyclic reactions have been studied extensively since Woodward and Hoffmann's seminal articles in 1965.[52] The cycloaddition behavior of phosphenium cations is well-documented,[14] including reactions with 1,3-dienes which give phospholenium cations **24**, and on the basis

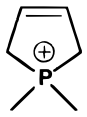

24

of a number of stereospecific experimental results, Cowley proposed that the reaction proceeds via a [2 + 4] disrotatory cheletropic mechanism.[53] The observed products in the reaction of carbenes,[54] silylenes, germylenes,[12,54,55] and stannylenes with 1,3-dienes[54−56] are similar. However, data for the cycloaddition reactivity of heavier low coordinate pnictogen species are limited.[57] Cations **7′** and **11′** are the only carbene analogues that have been observed to react with butadiene to form a Diels−Alder type product.[18,19]

The Diels−Alder (DA) reaction[58] is probably the most well-known pericyclic reaction and has been thoroughly investigated synthetically and theoretically.[59] The [2 + 2] and [4 + 2] cycloaddition reactivity of methylene has been studied theoretically;[60] however, despite the

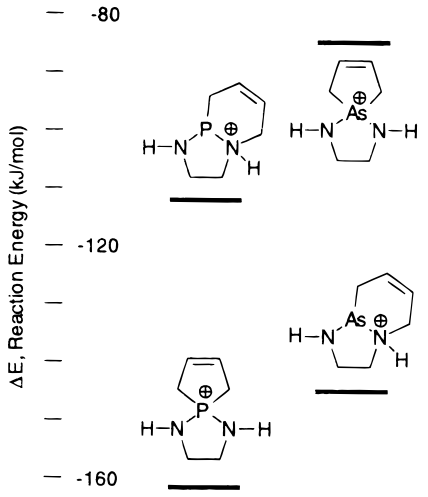

Figure 4. Schematic representation of reaction energies for the cycloaddition of **3** or **7** with *trans*-1,3-butadiene.

dramatic contrasts which are definitively experimentally demonstrated for phospholanium and arsolanium cations, we are unaware of *ab initio* studies for the cycloaddition behavior of pnictogenium cations. To model these reactions, we have optimized the structures of cycloaddition products **4**, **5**, **8**, and **9** and all minima were found to have the expected C_1 symmetry. Their single-point MP2 energies and ZPVE values are tabulated with those of cations **3** and **7** and those of *trans*-1,3-butadiene in Table 1. The structure of **9** is compared to that of **9′** in Figure 3. Reaction energies are listed in Table 8, and as illustrated schematically in Figure 4, the experimentally observed cycloaddition products for both **3′** and **7′** are calculated to be the thermodynamically favored product with respect to the other possible cycloaddition product in each system. Reaction of **3** to give **4** (−163.7 kJ/mol) and **5** (−112.2 kJ/mol) are both exothermic, but the Diels−Alder product **5** is more than 50 kJ/mol higher in energy. The theoretical model also mimics the experimental observations for arsolanium derivatives, predicting that the formation of **8** from **7** has a calculated reaction enthalpy of −85 kJ/mol, while the formation of arsonium **9** is more exothermic (−144.5 kJ/mol).

These conclusions validate the necessity of such a computational study, as a comparison of empirical bond energies ((all energies in kJ/mol) two P−C (552) bonds vs P−C (276) and C−N (314) and two As−C bonds (458) vs As−C (229) and C−N (314))[61] predict a DA-type product for both pnictogenium cations, but this has not even been observed in butadiene reactions with iminophosphines, which contain a formal P−N double bond.[62] Phosphorus and arsenic have nearly identical spectroscopic electronegativity values (P, 2.253, As, 2.211 Pauling units),[63] and the calculated charge distributions in **3** and **7** (*vide supra*) are not significantly different so that the contrasting cycloaddition behavior is not likely controlled by either property. One possible explanation arises from the different oxidation potentials of phos-

(51) Sauer, J.; Sustmann, R. *Angew. Chem., Int. Ed. Engl.* **1980**, *19*, 779−807 and references therein.
(52) (a) Woodward, R. B.; Hoffmann, R. *J. Am. Chem. Soc.* **1965**, *87*, 395−397. (b) Hoffmann, R.; Woodward, R. B. *J. Am. Chem. Soc.* **1965**, *87*, 2046−2048. (c) Woodward, R. B.; Hoffmann, R. *J. Am. Chem. Soc.* **1965**, *87*, 2511−2513. (d) Hoffmann, R.; Woodward, R. B. *J. Am. Chem. Soc.* **1965**, *87*, 4388−4389. (e) Hoffmann, R.; Woodward, R. B. *J. Am. Chem. Soc.* **1965**, *87*, 4389−4390.
(53) See for example: *Multiple Bonds and Low Coordination in Phosphorus Chemistry*; Regitz, M., Sherer, O. J., Eds.; Thieme: New York, 1990.
(54) Evanseck, J. D.; Mareda, J.; Houk, K. N. *J. Am. Chem. Soc.* **1990**, *112*, 73−80 and references therein.
(55) See for example: Tokitoh, N.; Kishikawa, K.; Matsumoto, T.; Okazaki, R. *Chem. Lett.* **1995**, 827−828.
(56) For example: Saito, M.; Tokitoh, N.; Okazaki, R. *Chem. Lett.* **1996**, 265−266.
(57) Review of arsaalkene and arsaalkynes: Weber, L. *Chem. Ber.* **1996**, *129*, 367−379.
(58) Diels, O.; Alder, K. *Justus Liebigs Ann. Chem.* **1928**, *460*, 98−122.
(59) Houk, K. N.; González, J.; Li, Y. *Acc. Chem. Res.* **1995**, *28*, 81−90.
(60) See for example: Houk, K. N.; Li, Y.; Evanseck, J. D. *Angew. Chem., Int. Ed. Engl.* **1992**, *31*, 682−708 and references therein.
(61) Mean bond enthalpies from: Elschenbroich, C.; Salzer, A. *Organometallics*, 2nd ed.: VCH: New York, 1992; p 11.
(62) Niecke, E. In *Multiple Bonds and Low Coordination in Phosphorus Chemistry*; Regitz, M., Sherer, O. J., Eds.; Thieme: New York, 1990; pp 293−320.
(63) Allen, L. C. *J. Am. Chem. Soc.* **1989**, *111*, 9003−9014.

phorus and arsenic. Whereas phosphorus(III) oxidizes preferentially to the P(V) state (*ca.* −50 kJ/mol), the corresponding oxidation of arsenic(III) is unfavorable (*ca.* +100 kJ/mol); thus, formal oxidation product **8** is unstable with respect to structural isomer **9**.[64] *Ab initio* calculations of the reaction $PnH_3 + H_2 \rightarrow PnH_5$ give ΔH values of 189.5 (P), 228.4 (As), 210.0 (Sb) and 305.4 (Bi) kJ/mol and correctly predict that As(V) and Bi(V) are significantly less favorable than P(V).[65] The relative instability of the As(V) oxidation state is due to the "d-block contraction" and results in the preferential formation of the adduct with the tricoordinate arsenic center. The Pn(III) to Pn(V) oxidation for antimony (*ca.* +100 kJ/mol) and bismuth (*ca.* +300 kJ/mol)[64] leads to the prediction that bismuthenium and possibly stibenium cations will also react in a fashion similar to that for the arsenium cations; however, these reactions have not as yet been examined experimentally. Unambiguous prediction is not possible for antimony, because the atom is more readily oxidized than either As or Bi and thus may form cheletropic adducts.

The rapid, quantitative, and regiospecific reactions observed experimentally imply concerted reaction mechanisms; thus, symmetries of the calculated frontier orbitals were examined in this context. The frontier orbitals that we have determined for cations **3** and **7** are consistent with previous results[29] and correspond to an "allylic-type" π-system with the additional σ_n nonbonding (A in C_2, A_1 in C_{2v}) MO (the lone pair) lower in energy than the π_n HOMO (A in C_2, A_2 in C_{2v}). As such, these systems cannot be considered truly isolobal with singlet carbenes which feature a σ_n HOMO.[6] Of the possible frontier orbital interactions, only that of the diene HOMO and pnictogenium LUMO is allowed. Although the A symmetry of the pnictogen lone pair MO (HOMO-1) is the same as that of the HOMO, the large energy difference between the HOMO and HOMO-1 (182.0 kJ/mol for **3**, 207.9 kJ/mol for **7**) and the node at the Pn center in the HOMO precludes a contribution of the lone pair in the frontier interaction (although orbital mixing is still a possibility). The π-type and lone pair frontier orbital interactions are qualitatively illustrated in Figures 5 and 6 and are consistent with both cheletropic and Diels−Alder type mechanisms involving the diene HOMO and the pnictolanium LUMO, while neither mechanism has a symmetry-allowed diene-LUMO−ene-HOMO interaction. If the lone pair molecular orbital (HOMO-1) is used in the frontier orbital interactions instead of the true ene HOMO (as for carbenes),[6] it becomes apparent that both HOMO−LUMO interactions (diene−pnictolanium and pnictolanium−diene) are of the appropriate symmetry for bond formation.

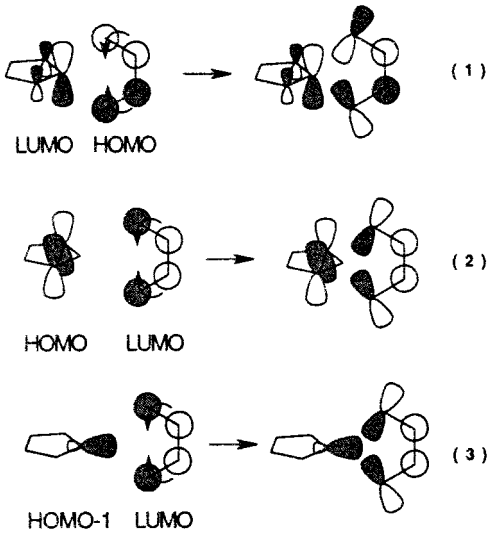

Figure 5. Frontier orbital interactions for the cheletropic mechanism of pnictolanium−diene cycloaddition.

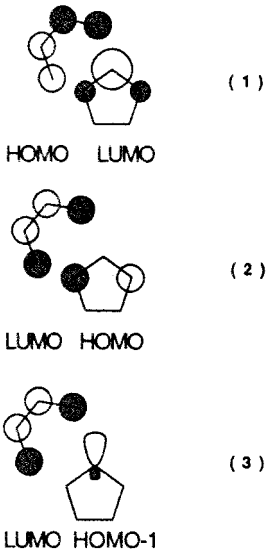

Figure 6. Frontier orbital interactions for the Diels−Alder type mechanism of pnictolanium−diene cycloaddition (viewed from above with butadiene plane above that of pnictolanium).

Conclusions

Diazapnictogenium cations are calculated to have singlet ground states, in agreement with experimental observations and consistent with previous calculations on structurally simpler acyclic cations, while the calculated models of the triplet species are in contrast with those of previous theoretical studies. HF/6-311G* geometry optimizations (gas phase) accurately predict the molecular structures of **3′**, **9′**, **10′**, and **11′**, which were previously determined experimentally by X-ray crystallography.

Dimerization reactions of cyclic diazapnictogenium cations are predicted to be unfavorable in the gas phase because of the requisite distortion of the stable monomeric forms. These conclusions are based on the energetics of the cations obtained from *ab initio* calculations and ignore all interactions such as those with the anions or solvent that are found in condensed phases. The experimentally observed dimer of the arsolanium cation **7′** is concluded to be a crystal-packing phenomenon which is likely dominated by the large difference in crystal lattice energy between (+1)(−1) salts and $(+2)(-1)_2$ salts.

(64) Phillips, C. S. G.; Williams, R. J. P. *Inorganic Chemistry*; Oxford University Press: London, 1966; Vol. 1, pp 632−638.

(65) Given values are from MP4/ECP calculations in: Moc, J.; Morokuma, K. *J. Am. Chem. Soc.* **1995**, *117*, 11790−11797. See also: Nagase, S. In *The Chemistry of Organic Arsenic, Antimony and Bismuth Compounds*; Patai, S., Ed.; Wiley: New York, 1994; pp 17−21 and references therein.

(66) In all tables the following format is used: **compound number** multiplicity label (s, singlet; d, doublet; t, triplet) symmetry (numbered when more than one structure of that symmetry).

More importantly, the dramatic contrast observed in the quantitative butadiene cycloaddition reactions of phosphenium (formal cheletropic cycloaddition → phosphonium cation) and arsenium (formal Diels−Alder cycloaddition → arsinoammonium cation) cations have been modeled by determining the absolute energies of structures **3**, **4**, **5**, **7**, **8**, and **9** (UMP2/6-311G*//UHF/6-311G* + 0.90 ZPVE). The relative energies of cycloaddition products **4** and **5** (52 kJ/mol) and **8** and **9** (−59 kJ/mol) are consistent with the experimental observations and indicate that the observed products are thermodynamically favored in each case. The anomalous butadiene cycloaddition behavior of arsenium cations is rationalized in terms of the relative instability of the As(V) oxidation state. The theoretical data obtained do not allow for analysis of the mechanism of the reactions of **3** or **7**, and it is possible that arsenium cations react with dienes to form spirocyclic adducts (**8**), which rapidly rearrange to the thermodynamically favored DA-type adducts (**9**).

Acknowledgment. We thank the Killam Trust and the Natural Sciences and Engineering Research Council of Canada (NSERC) for scholarships (C.L.B.M.) and the NSERC for funding (R.J.B., N.B.). We also thank the reviewers for helpful suggestions.

Supporting Information Available: Tables giving selected structural parameters from HF/6-311G* optimized geometries, Mulliken and NBO charge distributions, and calculated spin densities (11 pages). Ordering information is given on any current masthead page.

OM980126T